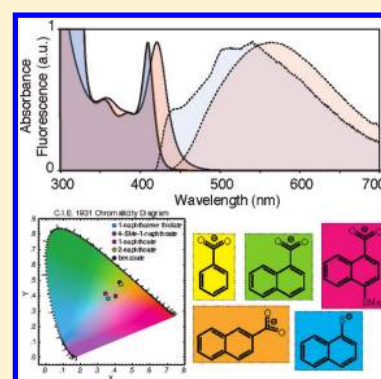


## Tuning the Surface Structure and Optical Properties of CdSe Clusters Using Coordination Chemistry

Brandi M. Cossairt,<sup>†</sup> Pavol Juhas,<sup>‡</sup> Simon J. L. Billinge,<sup>‡,§</sup> and Jonathan S. Owen<sup>\*,†</sup><sup>†</sup>Department of Chemistry, Columbia University, Havemeyer Hall, MC 3121, 3000 Broadway, New York, New York 10027, United States<sup>‡</sup>Department of Applied Physics and Applied Mathematics, Columbia University, New York, New York 10027, United States<sup>§</sup>Condensed Matter Physics and Materials Science Department, Brookhaven National Laboratory, Upton, New York 11973, United States

## S Supporting Information

**ABSTRACT:** A series of nonstoichiometric CdSe clusters with lowest energy electronic absorptions between 409 and 420 nm has been prepared from cadmium 1-naphthoate, 2-naphthoate, 4-thiomethyl-1-naphthoate, and 1-naphthalene thiolate complexes and diphenylphosphine selenide (DPPSe). Pair distribution function analysis of X-ray diffraction data, ligand exchange experiments, and NMR molecular weight analyses suggest the nanocrystal core changes minimally among these clusters despite significant changes to their absorption and luminescence spectra. Photoluminescence excitation spectra obtained at 77 K reveal an energy transfer process between the surface-trapped excited state and the naphthalene-containing ligands that leads to ligand phosphorescence. A Dexter energy transfer mechanism is proposed to explain the observation of ligand phosphorescence on excitation of the cluster. These compounds demonstrate that cluster absorption and trap luminescence can be controlled with surface coordination chemistry.

**SECTION:** Nanoparticles and Nanostructures

Magic sized clusters of cadmium selenide have been documented in numerous recent reports and are believed to play crucial roles in nanocrystal synthesis,<sup>1–11</sup> including as a solute reservoir for larger nanocrystals and as building blocks for the assembly of sheet and ribbon structures.<sup>1,12</sup> Many of these studies report a cluster with lowest energy absorption near 420 nm. Based on the energy of the 420 nm transition and a variety of other analytical techniques, including mass spectrometry, a structure with ~1.5 nm dimensions and a molecular formula of (CdSe)<sub>33–34</sub> has been proposed.<sup>10,12</sup> A nonstoichiometric formula, Cd<sub>35</sub>Se<sub>28</sub>, with a carboxylate and amine ligand shell has also been proposed.<sup>9</sup> All of these clusters show very similar absorption spectra, although a variety of surfactants and starting cadmium and selenium sources have been used in their preparation.

These clusters are characterized by broad photoluminescence line widths originating from radiative recombination of a surface-trapped exciton.<sup>4,11,13</sup> This assignment agrees well with previous studies of trap luminescence in other II–VI nanocrystals.<sup>13–15</sup> The Stokes shift and line width of the luminescence are expected to depend on the coordination chemistry of the cluster surface, both by influencing the energy of the trapped exciton and by modulating the coupling to the vibrational states that broaden the spectrum. For example, Rosenthal suggested that a particular emission feature at 440 nm from CdSe clusters is related to the interaction of phosphonic acid with the clusters surface because its energy

was invariant with the particle size.<sup>16</sup> This suggests that coordination chemistry can be used to tailor cluster luminescence spectra, and perhaps increase the photoluminescence quantum yield, which is as high as 11% for clusters with carboxylate and amine ligands.<sup>9,17</sup>

In the present study we use coordination chemistry to tune the steric and electronic environment at the cluster's surface, including the surface electronic states responsible for the trap luminescence. Both the absorption and photoluminescence spectra of the clusters are sensitive to the steric and electronic nature of the anionic (carboxylate or thiolate) ligand in a way that is not readily explained by a change in cluster size. We have also identified a Dexter energy transfer process between the surface trapped excited state of the clusters and the naphthalene carboxylate and thiolate ligands bound to its surface.

We previously utilized benzoate and amine ligands to crystallize a CdSe cluster and proposed a molecular formula [(CdSe)<sub>4</sub>(Cd(O<sub>2</sub>C–C<sub>6</sub>H<sub>5</sub>)<sub>2</sub>)(H<sub>2</sub>NC<sub>12</sub>H<sub>25</sub>)<sub>2</sub>]<sub>7±1</sub> on the basis of Rutherford backscattering spectrometry, NMR spectroscopy of the ligand shell, and solution molecular weight measurements.<sup>9</sup> In the present study we utilize this synthesis to prepare and isolate clusters in which excess cadmium ions balance charge with several naphthalene containing X-type ligands, including 1-

Received: October 13, 2011

Accepted: November 22, 2011

Published: November 22, 2011

naphthoate, 2-naphthoate, 4-thiomethyl-1-naphthoate, and 1-naphthalene thiolate. Specifically, combining  $\text{Cd}(\text{X})_2$ , prepared from  $\text{CdO}$  or  $\text{CdMe}_2$ , and the free acid ( $\text{HX}$ ), with dodecylamine (DDA) and diphenylphosphine selenide (DPPSe) at 45 °C resulted in slow changes to the UV–visible spectra of aliquots indicative of cluster growth (Figure 1).

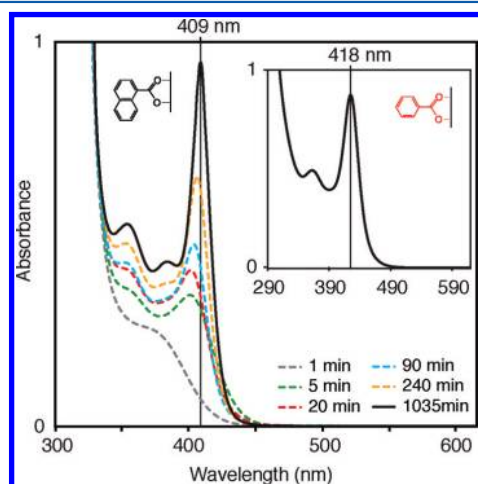


**Figure 1.** Growth profile (absorbance) of 1-naphthoate-capped particles at 45 °C in toluene. Heating beyond 1035 min did not result in any further changes in position or breadth of the lowest energy electronic transition. The absorption spectrum for benzoate-capped particles grown under the same conditions is shown in the inset.

These changes were significantly slower for reactions involving cadmium 1-naphthoate (17 h) than in syntheses using cadmium benzoate (2 h). We hypothesize that a slower crystallization rate is a result of steric hindrance at the growing particle surface because conversion of DPPSe to the tetraphenyldiphosphine ( $^{31}\text{P}$  –14.5 ppm) and *N*-dodecyl-diphenylphosphinamide selenide ( $^{31}\text{P}$  57.3 ppm) coproducts does not limit the rate of cluster formation in both cases.<sup>18</sup>

Both the absorption and photoluminescence spectra vary with changes to the ligand structure. 1-Naphthoate-derived clusters display a lowest energy electronic transition at 409 nm and more narrow absorption features (fwhm = 14 nm) when compared to the others, in particular the benzoate-derived cluster ( $\lambda = 418$  nm, fwhm = 28 nm) (Figure 1, inset). Clusters derived from 2-naphthoate, 4-thiomethyl-1-naphthoate, and 1-naphthalene thiolate have the lowest energy electronic transitions that fall between these extremes (Figure 2A). In all cases, the room-temperature photoluminescence spectra are broad and have significant Stokes shifts (>0.75 eV), indicative of trap luminescence (Figures 2B and 3). For example, the benzoate-terminated sample, excited at 410 nm, exhibits a broad luminescence spectrum with a peak maximum at 560 nm and no observable fine structure. The 1-naphthoate-terminated sample shows a broad but featured spectrum with a peak maximum at 550 nm. The luminescence spectrum of the 2-naphthoate-derived cluster is similar in shape to the spectrum of benzoate cluster, although additional ligand-derived features are also observed (see below). Unlike the benzoate-terminated cluster, the quantum yield of the 1-naphthoate-terminated particles is strongly dependent on the concentration of free amine and ranges from 1% to 11% (see Figure 1S in the

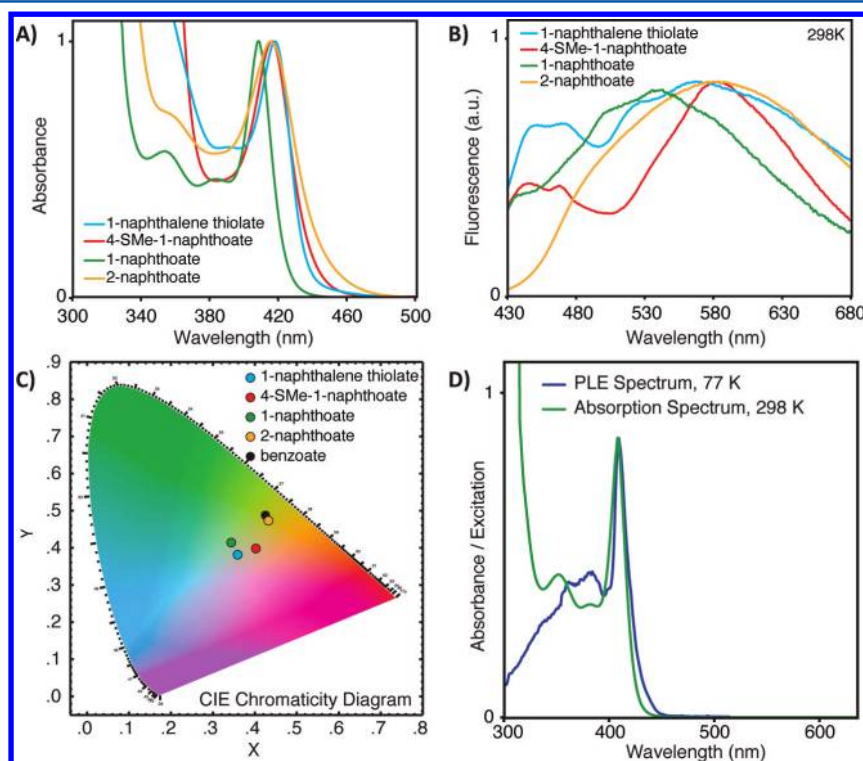


**Figure 2.** Absorption (A) and photoluminescence spectra ( $\lambda_{\text{excitation}} = 410$  nm) (B) for 1-naphthoate, 2-naphthoate, 4-SMe-1-naphthoate, and 1-naphthalene thiolate-capped particles at 298 K. (C) CIE chromaticity coordinates for 1-naphthoate, 2-naphthoate, 4-SMe-1-naphthoate, and 1-naphthalene thiolate-capped particles at 298 K. (D) Photoluminescence excitation spectrum ( $\lambda_{\text{emission}} = 540$  nm,  $\lambda_{\text{excitation}} = 300$  to 520 nm) for 1-naphthoate-capped particles at 77 K plotted with the corresponding absorption spectrum at 298 K.

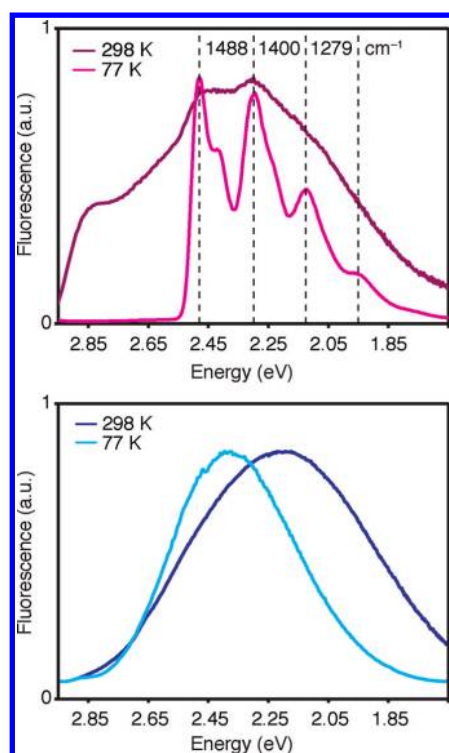


**Figure 3.** Fluorescence spectra for 1-naphthoate (top) and benzoate (bottom) capped particles at 298 and 77 K plotted in eV. The frequencies marked in the 1-naphthoate spectra represent peak separations in  $\text{cm}^{-1}$ , reflecting vibrational coupling to the  $\pi$  system of the naphthalene unit.

Supporting Information).<sup>19</sup> This may reflect a weaker amine binding and concentration-dependent surface coverage caused by the steric bulk of the 1-naphthoate ligands.  $^1\text{H}$  NMR spectra of the isolated clusters also reflect this behavior, where the ratio of amine to naphthoate is less than 1:1 as determined by NMR integration in all isolated 1-naphthoate samples (see Table 1 and Figure 3S in the Supporting Information).<sup>20</sup>

Photoluminescence spectra of the naphthoate and naphthalene thiolate ligated clusters are strongly featured, including transitions at the low-energy end of the band that are coincident with phosphorescence of the free ligands (see below). Any luminescence from the ligand must be stimulated by excitation of the cluster because ligand absorption sets in at much shorter wavelengths than 410 nm, where the cluster was excited to obtain the spectra in Figure 2B. At the high-energy end of the spectrum ( $\lambda < 480$  nm), the position of the absorption features correlates with changes to the lowest energy absorption maxima as the ligand is changed. These spectral features are reminiscent of those visible in spectra reported by Rosenthal and attributed to surface trap state pinning.<sup>16</sup> The

emission color of the clusters is plotted using CIE chromaticity coordinates in Figure 2C,<sup>21</sup> clearly showing that the various ligands allow the luminescence color to be tuned.

Changes in the fluorescence line shape were further investigated by acquiring photoluminescence spectra at 77 K in a liquid nitrogen-cooled quartz Dewar ( $\lambda_{\text{excitation}} = 410$  nm) (Figure 3). The luminescence from the benzoate-derived cluster blue shifts and narrows upon cooling, behavior characteristic of an excited state coupled strongly to vibrations,<sup>22,23</sup> and luminescence from the 1-naphthoate-terminated samples is replaced by a spectrum characteristic of naphthalene phosphorescence.<sup>24</sup> A photoluminescence excitation spectrum (Figure 2D) measured at 77 K shows that cluster excitation leads to ligand phosphorescence, suggesting the surface-trapped excited state sensitizes the naphthalene triplet.<sup>25–28</sup> These features from naphthalene phosphorescence (500, 539, 583, and 631 nm) overlap with the trap luminescence at room temperature. Photoluminescence spectra acquired at 77 K for the 4-thiomethyl-1-naphthoate, 1-naphthalene thiolate, and 2-naphthoate-terminated particles also show bright naphthalene-derived phosphorescence (see Figure 3S in the Supporting Information).

The phosphorescence observed at 77 K indicates an efficient energy transfer process between the trapped excited state and the ligand  $\pi$ -system.<sup>29</sup> Triplet–triplet energy transfer is spin-forbidden by the Förster transfer mechanism<sup>30,31</sup> and can proceed instead by an electron exchange mechanism known as Dexter energy transfer. This occurs by a through-bond process,<sup>32</sup> wherein electrons are exchanged in a correlated manner between the HOMOs and LUMOs of the donor and the acceptor, specifically between triplet states of the surface-trapped excited state and the naphthalene ligands in our system.<sup>30,33</sup> Such a mechanism requires the donor and the acceptor to be within 10 Å of one another because the efficiency of the energy transfer falls off exponentially with distance.<sup>30–32</sup> This short-range energy transfer is expected to be quite facile in our system where carboxylate ligands bind the cluster surface in a bidentate fashion,<sup>9</sup> separating the naphthalene unit from the clusters surface by only three bonds.<sup>34</sup> A scheme depicting surface electron trapping followed by energy transfer is shown in Scheme 1. At room temperature, we see both naphthoate phosphorescence and cluster trap emission, suggesting that the rates for Dexter energy transfer and emission from the trap state are comparable. At low temperature however, the rate of Dexter energy transfer is dominant and only naphthalene-based phosphorescence is observed (Figure 3). This may be explained by a more favorable relative orientation of the donor and the acceptor,<sup>31</sup> and by an increase in trap-state lifetime at low temperature.<sup>14</sup>

A number of experiments indicate that the CdSe core is preserved among the series of benzoate and naphthoate-ligated

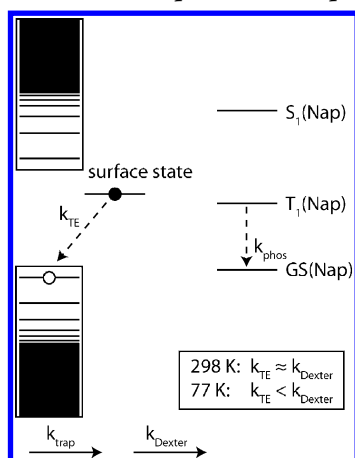
**Table 1.**  $^1\text{H}$  NMR Study Quantifying the Amount of X-Type Ligand and DDA in a Known Mass of Isolated Nanoclusters Using Ferrocene As an Internal Standard<sup>a</sup>

X	mass clusters	Fc (10 H): DDA (23 H)	actual mmol DDA	X: DDA	mmol X	theoretical mw	calculated mmol X	accuracy
1-naphthoate	50 mg	1: 270 0.355 $\mu\text{mol}$ Fc	0.042 mmol	1.7: 1	0.071 mmol	10024 g/mol	0.070 mmol	98.7%
2-naphthoate	50 mg	1: 341 0.222 $\mu\text{mol}$ Fc	0.033 mmol	2: 1	0.066 mmol	9839 g/mol	0.071 mmol	92.9%
4-SMe-1-naphthoate	50 mg	1: 342 0.222 $\mu\text{mol}$ Fc	0.033 mmol	2: 1	0.066 mmol	10316 g/mol	0.067 mmol	98.5%
1-HS-naphthoate	50 mg	1: 251 0.355 $\mu\text{mol}$ Fc	0.039 mmol	1.8: 1	0.070 mmol	9440 g/mol	0.074 mmol	94.6%

<sup>a</sup>Calculated weights are based on the formula  $\text{Cd}_{35}\text{Se}_{28}[(\text{X})_{14}(\text{H}_2\text{NC}_{12}\text{H}_{25})_n]$ , where  $n$  is determined from the ratio of X-type ligand to DDA in the sample. Errors in the measured mmol using  $^1\text{H}$  NMR integration are estimated to be below 10%.



**Scheme 1. Model for the Two Possible Radiative Pathways in  $\text{Cd}_{35}\text{Se}_{28}$  Nanoclusters with 1-Naphthoate Ligands, Where  $k_{\text{trap}}$  Is the Rate of Exciton Self-Trapping,  $k_{\text{Dexter}}$  Is the Rate of Dexter Energy Transfer,  $k_{\text{TE}}$  Is the Rate of Trap Emission, and  $k_{\text{phos}}$  Is the Rate of 1-Naphthoate Phosphorescence<sup>a</sup>**



<sup>a</sup>At room temperature,  $k_{\text{TE}}$  is approximately equal to  $k_{\text{Dexter}}$ , but at low temperature,  $k_{\text{Dexter}}$  is dominant.

clusters, despite clear differences in their absorption and fluorescence spectra.<sup>35</sup> For example, pair distribution functions (PDFs), obtained from the Fourier transform of the powder X-ray diffraction data, for the benzoate and 1-naphthoate-derived clusters are essentially indistinguishable, implying a similar structure (Figure 4).<sup>36,37</sup> Changes to the empirical formula,

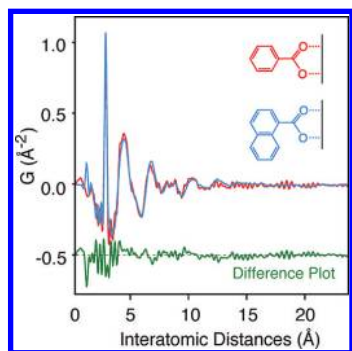


**Figure 4.** PDF data measured by powder XRD from 1-naphthoate (blue) and benzoate (red) capped particles. The green line is the difference between the two curves.

$[(\text{CdSe})_4(\text{Cd}(\text{O}_2\text{C}-\text{C}_6\text{H}_5)_2)(\text{H}_2\text{NC}_{12}\text{H}_{25})_2]_{7\pm1}$ , on changing the X-type ligand were also measured using  $^1\text{H}$  NMR spectroscopy. Fifty milligrams of each cluster were dissolved in  $d_6$ -benzene and the concentration of organic ligands was determined using an internal standard. Comparing the measured ligand concentration with the expected value for a cluster with empirical formula  $[(\text{CdSe})_4(\text{Cd}(\text{O}_2\text{C}-\text{C}_6\text{H}_5)_2)(\text{H}_2\text{NC}_{12}\text{H}_{25})_2]_{7\pm1}$ , matched the theoretical value within the error of the measurement in all cases (Table 1).<sup>38</sup>

Finally, ligand exchange reactions indicate that the as-grown 1-naphthoate cluster is a structural isomer of the other clusters. Ligand exchange was performed on the 1-naphthoate terminated clusters by combining them with 1–20 equiv of dodecylammonium benzoate or 1–20 equiv of tri-*n*-butylphosphine per cluster at room temperature. UV-vis spectroscopy allowed monitoring of the exchange process in situ where a

gradual red shift and broadening occurred upon addition of the ligand, eventually leading to a spectrum characteristic of the benzoate cluster (Figure 5, 1 equiv tri-*n*-butylphosphine).

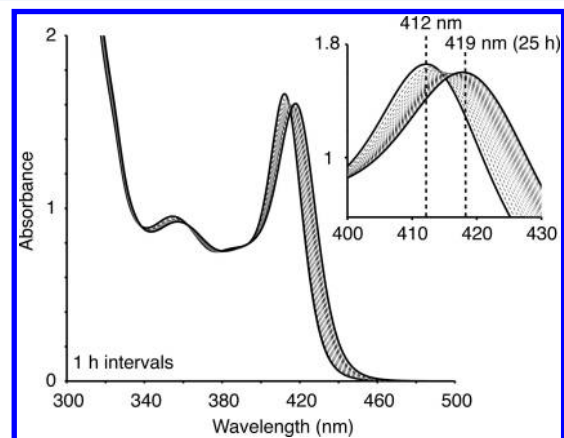


**Figure 5.** UV-vis traces for the reaction between 1-naphthoate-capped particles and 1 equiv tributylphosphine at 298 K (spectra acquired in 1 h intervals). The inset is a zoom in of the region of the absorbance maximum, which depicts the smooth red shift over time.

Changes were also visible in the photoluminescence spectrum, where the peak maximum ultimately shifted to longer wavelengths. Increasing the concentration of added carboxylate or phosphine caused more rapid changes, although the final absorption and photoluminescence spectra are the same in all cases.  $^1\text{H}$  NMR spectroscopy suggests that ligand exchange is more rapid than changes to the optical spectra because a mixture of free and bound carboxylates display a single set of broadened NMR peaks, consistent with ligand exchange more rapid than the NMR time scale (see Figure S5 in the Supporting Information). On the other hand, the reverse exchange reaction, beginning with benzoate-derived clusters and 20 equiv dodecylammonium 1-naphthoate, does not cause the UV-vis spectrum to blue shift. Nanocrystals isolated from this reaction display  $^1\text{H}$  NMR spectroscopic features characteristic of surface bound naphthoate rather than benzoate ligands. (see Figure 4S in the Supporting Information).

These results suggest that a structural reorganization of the as synthesized 1-naphthoate-derived cluster causes the lowest energy absorption to shift from 409 to 420 nm. Displacement of the 1-naphthoate ligands by benzoate might cause a structural relaxation of the cluster by relieving the steric influence of the 1-naphthoate. On the other hand, 1 equiv of tri-*n*-butylphosphine causes the conversion of the starting to final structure without exchanging the 1-naphthoate ligands. In addition, exchanging the benzoate ligands for 1-naphthoate does not produce a corresponding spectral blue shift. As a result, we believe the structure formed from cadmium 1-naphthoate and DPPSe is likely a kinetic product that is energetically uphill from the structure made from cadmium benzoate or the clusters with the spectra shown in Figure 2A. Furthermore, the smooth red shift seen in the lowest energy absorption maximum during the ligand exchange experiments, rather than isosbestic behavior, particularly with tri-*n*-butylphosphine, indicates there are a distribution of intermediate structural isomers that contribute to the position and breadth of the spectra of these compounds. Such changes must be subtle variations in the structure that are not clearly visible in the PDF and perhaps arise from changes to the coordination

geometries of surface atoms. Evidence for such surface-functionalization-dependent excitonic absorption features has recently been provided in a study of larger II–VI semiconductor nanocrystals.<sup>39</sup>

In conclusion, we have synthesized cadmium selenide clusters stabilized by a series of naphthoate and naphthalene thiolate surface ligands. The results of atomic PDF analysis, ligand exchange reactions, and molecular weight analysis support a series of clusters with the same core formula, whose optical transitions are influenced by the steric profile of the ligands. In the case of 1-naphthoate, steric encumbrance leads to crystallization of a higher energy structure that can be isomerized by the addition of phosphine or carboxylate ligands. This has important implications for quantum dot analysis more generally, as the traditional sizing formulas<sup>40–42</sup> do not take into account any surface or ligand effects, which have important consequences for the energy and shape of the lowest energy electronic transition at small sizes.<sup>43</sup> Photoluminescence spectra obtained at 77 K show the broad cluster emission is replaced by ligand phosphorescence, suggesting efficient energy transfer between a surface trapped excited state and a naphthalene triplet state via a through-bond Dexter transfer mechanism. Ligand phosphorescence also contributes to the luminescence at room temperature, resulting in spectra that are sensitive to the ligand structure as well as the geometry of the core. Together these results highlight the important role of surface chemistry in tailoring the optical properties of small nanocrystals, opening up further avenues for their exploration in lighting and biological sensing applications.

## ■ ASSOCIATED CONTENT

### ■ Supporting Information

Details concerning experimental procedures, instrumentation, and additional characterization can be found in the Supporting Information document accompanying this text. This material is available free of charge via the Internet at <http://pubs.acs.org>.

## ■ AUTHOR INFORMATION

### Corresponding Author

\*E-mail: [jso2115@columbia.edu](mailto:jso2115@columbia.edu).

## ■ ACKNOWLEDGMENTS

B.M.C. thanks the NIH for postdoctoral funding via an NRSA Grant 10484140. Photophysical and atomic pair distribution function studies are supported as part of the Center for Redefining Photovoltaic Efficiency Through Molecule Scale Control, an Energy Frontier Research Center funded by the U.S. Department of Energy, Office of Science, Office of Basic Energy Sciences under Award Number DE-SC0001085. J.S.O. thanks 3M Corporation for a nontenured faculty grant in support of this work. Use of the Advanced Photon Source, an Office of Science User Facility operated for the U.S. Department of Energy (DOE) Office of Science by Argonne National Laboratory, was supported by the U.S. DOE under Contract No. DE-AC02-06CH11357. Use of the National Synchrotron Light Source, Brookhaven National Laboratory, was supported by the U.S. DOE under Contract No. DE-AC02-98CH10886.

## ■ REFERENCES

(1) Jiang, Z. J.; Kelley, D. F. Role of Magic-Sized Clusters in the Synthesis of CdSe Nanorods. *ACS Nano* **2010**, *4* (3), 1561–1572.

(2) Yu, K.; Hu, M. Z.; Wang, R.; Le Piolet, M.; Frotey, M.; Zaman, B.; Wu, X.; Leek, D. M.; Tao, Y.; Wilkinson, D.; et al. Thermodynamic Equilibrium-Driven Formation of Single-Sized Nanocrystals: Reaction Media Tuning CdSe Magic-Sized versus Regular Quantum Dots. *J. Phys. Chem. C* **2010**, *114*, 3329–3339.

(3) Kudera, S.; Zanella, M.; Giannini, C.; Rizzo, A.; Li, Y.; Gigli, G.; Cingolani, R.; Ciccarella, G.; Spahl, W.; Parak, W. J.; et al. Sequential Growth of Magic-Size CdSe Nanocrystals. *Adv. Mater.* **2007**, *19*, 548–552.

(4) Bowers, M. J. I.; McBride, J. R.; Rosenthal, S. J. White-Light Emission from Magic-Sized Cadmium Selenide Nanocrystals. *J. Am. Chem. Soc.* **2005**, *127*, 15378–15379.

(5) Chen, H. S.; Kumar, R. V. Discontinuous Growth of Colloidal CdSe Nanocrystals in the Magic Structure. *J. Phys. Chem. C* **2009**, *113*, 31–36.

(6) Dai, Q.; Li, D.; Chang, J.; Song, Y.; Kan, S.; Chen, H.; Zou, B.; Xu, W.; Xu, S.; Liu, B.; et al. Facile Synthesis of Magic-Sized CdSe and CdTe Nanocrystals with Tunable Existence Periods. *Nanotechnology* **2007**, *18*, 405603–7.

(7) Dukes, A. D. I.; McBride, J. R.; Rosenthal, S. J. Synthesis of Magic-Sized CdSe and CdTe Nanocrystals with Diisooctylphosphinic Acid. *Chem. Mater.* **2010**, *22* (22), 6402–6408.

(8) Ouyang, J.; Zaman, B.; Yan, F. J.; Johnston, D.; Li, G.; Wu, X.; Leek, D.; Ratcliffe, C. I.; Ripmeester, J. A.; Yu, K. Multiple Families of Magic-Sized CdSe Nanocrystals with Strong Bandgap Photoluminescence via Noninjection One-Pot Syntheses. *J. Phys. Chem. C* **2008**, *112*, 13805–13811.

(9) Cossairt, B. M.; Owen, J. S. CdSe Clusters: At the Interface Between Small Molecules and Quantum Dots. *Chem. Mater.* **2011**, *23*, 3114–3119.

(10) Kasuya, A.; Sivamohan, R.; Barnakov, Y. A.; Dmitruk, I. M.; Nirasawa, T.; Romanyuk, V. R.; Kumar, V.; Mamykin, S. V.; Tohji, K.; Jeyadevan, B.; et al. Ultra-Stable Nanoparticles of CdSe Revealed from Mass Spectrometry. *Nat. Mater.* **2004**, *3*, 99–102.

(11) McBride, J. R.; Dukes, A. D. I.; Schreuder, M. A.; Rosenthal, S. J. On Ultrasmall Nanocrystals. *Chem. Phys. Lett.* **2010**, *498*, 1–9.

(12) Liu, Y.-H.; Wang, F.; Wang, Y.; Gibbons, P. C.; Buhro, W. E. Lamellar Assembly of Cadmium Selenide Nanoclusters into Quantum Belts. *J. Am. Chem. Soc.* **2011**, *133* (42), 17005–17013.

(13) Bowers, M. J. I.; McBride, J. R.; Garrett, M. D.; Sammons, J. A.; Dukes, A. D. I.; Schreuder, M. A.; Watt, T. L.; Lupini, A. R.; Pennycook, S. J.; Rosenthal, S. J. Structure and Ultrafast Dynamics of White-Light-Emitting CdSe Nanocrystals. *J. Am. Chem. Soc.* **2009**, *131*, 5730–5731.

(14) Chestnoy, N.; Harris, T. D.; Hull, R.; Brus, L. E. Luminescence and Photophysics of CdS Semiconductor Clusters. *J. Phys. Chem.* **1986**, *90*, 3393–3399.

(15) van Dijken, A.; Meulenkaamp, E. A.; Vanmaekelbergh, D.; Meijerink, A. The Kinetics of the Radiative and Nonradiative Processes in Nanocrystalline ZnO Particles upon Photoexcitation. *J. Phys. Chem. B* **2000**, *104*, 1715–1723.

(16) Dukes, A. D. I.; Schreuder, M. A.; Sammons, J. A.; McBride, J. R.; Smith, N. J.; Rosenthal, S. J. Pinned Emission from Ultrasmall Cadmium Selenide Nanocrystals. *J. Chem. Phys.* **2008**, *129*, 121102–4.

(17) Schreuder, M. A.; Xiao, K.; Ivanov, I. N.; Weiss, S. M.; Rosenthal, S. J. White Light-Emitting Diodes Based on Ultrasmall CdSe Nanocrystal Electroluminescence. *Nano Lett.* **2010**, *10* (2), 573–576.

(18) Conversion of the precursors is readily monitored with <sup>31</sup>P NMR spectroscopy, where phosphoramidate and tetraphenyldiphosphine byproducts are observed shortly after mixing.

(19) Photoluminescence quantum yields were determined using Coumarin-53 as an external reference.

(20) Unusually deshielded <sup>1</sup>H NMR features are visible between 0.1 and 0.6 ppm that may arise from close proximity of the methylene chains and the aromatic rings. See Supporting Information.

(21) Guild, J. The Colorimetric Properties of the Spectrum. *Philos. Trans. R. Soc. London, A* **1931**, *230*, 149–187.

- (22) Nirmal, M.; Murray, C. B.; Bawendi, M. G. Fluorescence-Line Narrowing in CdSe Quantum Dots: Surface Localization of the Photogenerated Exciton. *Phys. Rev. B* **1994**, *50* (4), 2293–2300.
- (23) Bawendi, M. G.; Steigerwald, M. L.; Brus, L. E. The Quantum Mechanics of Larger Semiconductor Clusters. *Annu. Rev. Phys. Chem.* **1990**, *41*, 447–496.
- (24) Hochstrasser, R. M. The Luminescence of Complex Molecules in Relation to the Internal Conversion of Excitation Energy. *Can. J. Chem.* **1961**, *39*, 1776–1782.
- (25) Rogach, A. L. Fluorescence Energy Transfer in Hybrid Structures of Semiconductor Nanocrystals. *Nano Today* **2011**, *6* (4), 355–365.
- (26) Jiang, G.; Susha, A. S.; Lutich, A. A.; Stefani, F. D.; Feldman, J.; Rogach, A. L. Cascaded FRET in Conjugated Polymer/Quantum Dot/Dye-Labeled DNA Complexes for DNA Hybridization Detection. *ACS Nano* **2009**, *3* (12), 4127–4131.
- (27) Kowanko, D.; Schuster, J.; Amecke, N.; Abdel-Mottaleb, M.; Dobrawa, R.; Wurthner, F.; von Borczyskowski, C. FRET and Ligand-Related Non-FRET Processes in Single Quantum Dot–Perylene Bisimide Assemblies. *Phys. Chem. Chem. Phys.* **2010**, *12*, 4112–4123.
- (28) Neither 1-naphthoic acid, dodecylammonium 1-naphthoate, nor cadmium naphthoate have significant absorption at wavelengths longer than 310 nm.
- (29) Coupling to the  $\pi$  system is indicated by the energy separation of the vibrational progression observed in the 77 K luminescence spectrum.
- (30) Lakowicz, J. R. *Principles of Fluorescence Spectroscopy*, 3rd ed.; Springer: New York, 2006; p 980.
- (31) Speiser, S. Photophysics and Mechanisms of Intramolecular Electronic Energy Transfer in Bichromophoric Molecular Systems. *Chem. Rev.* **1996**, *96*, 1953–1976.
- (32) Dexter, D. L. A Theory of Sensitized Luminescence in Solids. *J. Chem. Phys.* **1953**, *21*, 836–850.
- (33) Underwood, D. F.; Kippeny, T.; Rosenthal, S. J. Ultrafast Carrier Dynamics in CdSe Nanocrystals Determined by Femtosecond Fluorescence Upconversion Spectroscopy. *J. Phys. Chem. B* **2001**, *105*, 436–443.
- (34) Jackson, G.; Porter, G. Acidity Constants in the Triplet State. *Proc. R. Soc. London A* **1961**, *260* (1300), 13–30.
- (35) Frederick, M. T.; Weiss, E. A. Relaxation of Exciton Confinement in CdSe Quantum Dots by Modification with a Conjugated Dithiocarbamate Ligand. *ACS Nano* **2010**, *4* (6), 3195–3200.
- (36) Masadeh, A. S.; Bozin, E. S.; Farrow, C. L.; Paglia, G.; Juhas, P.; Billinge, S. J. L. Quantitative Size and Strain Determination of CdSe Nanoparticles using Atomic Pair Distribution Function Analysis. *Phys. Rev. B* **2007**, *76*, 115413–1–11.
- (37) The PDF allows convenient comparison between the core structures of a given pair of samples, as the organic surfactant shell contains only weakly scattering, light elements (C, H, N, O) whose signals contribute weakly to the diffraction signal.
- (38) Assuming a  $\text{Cd}_{35}\text{Se}_{28}$  core, 14 X-type ligands are required to maintain the clusters charge neutrality.
- (39) Chen, O.; Yang, Y.; Wu, H.; Niu, C.; Yang, J.; Cao, Y. C. Surface-Functionalization-Dependent Optical Properties of II–VI Semiconductor Nanocrystals. *J. Am. Chem. Soc.* **2011**, *133* (43), 17504–17512.
- (40) Jasieniak, J.; Smith, L.; van Embden, J.; Mulvaney, P. Re-examination of the Size-Dependent Absorption Properties of CdSe Quantum Dots. *J. Phys. Chem. C* **2009**, *113*, 19468–19474.
- (41) Leatherdale, C. A.; Woo, W. K.; Mikulec, F. V.; Bawendi, M. G. On the Absorption Cross Section of CdSe Nanocrystal Quantum Dots. *J. Phys. Chem. B* **2002**, *106*, 7619–7622.
- (42) Yu, W. W.; Qu, L.; Guo, W.; Peng, X. Experimental Determination of the Extinction Coefficient of CdTe, CdSe, and CdS Nanocrystals. *Chem. Mater.* **2003**, *15*, 2854–2860.
- (43) Sizing formulas indicate that nanocrystals with lowest energy absorption at 409 and 419 nm differ in volume by  $30 \text{ \AA}^3$ , about the volume of one cadmium atom.